

## Effects of Ni/Al<sub>2</sub>O<sub>3</sub> catalyst treatment condition on thermocatalytic conversion of spent disposable wipes

Hee Sue Lee<sup>\*,‡</sup>, Sungyup Jung<sup>\*,‡</sup>, Sung Woo Lee<sup>\*\*\*</sup>, Yong Tae Kim<sup>\*\*\*</sup>, and Jechan Lee<sup>\*,\*\*\*\*,†</sup>

\*Department of Global Smart City, Sungkyunkwan University, 2066 Seobu-ro, Suwon 16419, Korea

\*\*Department of Environmental Engineering, Kyungpook National University, 80 Daehak-ro, Daegu 41566, Korea

\*\*\*Chemical and Process Technology Division, Korea Research Institute of Chemical Technology, 141 Gajeong-ro, Daejeon 34114, Korea

\*\*\*\*School of Civil, Architectural Engineering, and Landscape Architecture, Sungkyunkwan University, 2066 Seobu-ro, Suwon 16419, Korea

(Received 21 February 2023 • Revised 14 March 2023 • Accepted 31 March 2023)

**Abstract**—Municipal solid waste (MSW) management is an essential municipal service. Proper waste treatment is an important part of the waste management. Thermocatalytic waste upcycling has recently gained great interest and attention as a method to extract value from waste, which potentially substitutes traditional waste treatment methods. This study aims at demonstrating the potential for thermocatalytic waste upcycling using spent disposable wipes as an MSW surrogate. Two different Ni/Al<sub>2</sub>O<sub>3</sub> catalysts were prepared, treated under two different atmospheres (N<sub>2</sub> and CO<sub>2</sub>). The catalyst treated in N<sub>2</sub> (Ni/Al<sub>2</sub>O<sub>3</sub>-N<sub>2</sub>) exhibited a higher surface metallic Ni site than the catalyst treated in CO<sub>2</sub> (Ni/Al<sub>2</sub>O<sub>3</sub>-CO<sub>2</sub>). The use of the Ni/Al<sub>2</sub>O<sub>3</sub>-N<sub>2</sub> increased the yield of gas pyrolysate and decreased the yield of byproduct (e.g., wax), compared with no catalyst and the Ni/Al<sub>2</sub>O<sub>3</sub>-CO<sub>2</sub>. In particular, the Ni/Al<sub>2</sub>O<sub>3</sub>-N<sub>2</sub> catalyst affected the generation of gaseous hydrogen (H<sub>2</sub>) by increasing the H<sub>2</sub> yield by up to 102% in comparison with the other thermocatalytic systems. The highest H<sub>2</sub> yield obtained with the Ni/Al<sub>2</sub>O<sub>3</sub>-N<sub>2</sub> was attributed to the most surface metallic Ni sites. However, the Ni/Al<sub>2</sub>O<sub>3</sub>-N<sub>2</sub> catalyst led to char having a lower higher heating value than the other catalysts due to its lowest carbon content. The results indicated that the reduction treatment environment for Ni/Al<sub>2</sub>O<sub>3</sub> catalyst influences thermocatalytic conversion product yields of spent disposable wipes, including enhanced H<sub>2</sub> production.

Keywords: Municipal Solid Waste, Waste Treatment, Thermochemical Conversion Process, Pyrolysis, Base Metal Catalyst

### INTRODUCTION

Since the living standard arising from world economy growth has significantly improved, interest in individual hygiene management has also grown [1]. In addition, the outbreak of COVID-19 expedited the use of disposable personal hygiene products [2]. Disposable wipes, also known as cleaning tissues, are among broadly used personal care and hygiene materials to clean dirty skin and a variety of materials [3]. The demand for disposal wipes is continuously increasing in household and different stores because their simple use, cheap price, robustness, convenience of storage, infection-prevention effect, and easiness of mass production [1]. Also, disposable wipes are heavily used in facial make-up as a cleaning purpose [4]. Because of the continuously increasing demand for disposal wipes, their global market size was valued at USD 21.5 billion and is projected to expand at an annual average growth rate of 3.6% by 2030 [5].

Despite the fact that disposal wipes improve the quality of life and

hygiene, the short life span and current treatment methods have been increasing the environmental problems to all the environment media (soil, river, and air) [6]. Disposable wipes look like paper and recyclable materials, but they are mixtures of plastics and natural polymers such polyester, polypropylene, cotton, wood pulp, or rayon fiber [7]. These are non-biodegradable substances that are not recyclable because of their complicated heterogeneity [8]. Disposable wipes are also one of the main causes of failure in sewage treatment plants, blocking sewage pipes and foreign substance treatment machines [9]. As such, disposable wipes are considered a general solid waste, and discarded into waste bins to be incinerated and landfilled [10]. Landfilling of disposable wipes can result in formation of microplastics into the soil and river when the landfilling site is not properly managed [11,12]. Natural weathering from the chemical reactions of plastic waste in soil, river, and sea under sunshine can degrade disposable plastics into microplastics physically and chemically [13]. Advanced countries manage the landfilling sites properly by installing a liner on the bottom of the piles of waste [14]. However, there are still a variety of landfilling sites, releasing leachates including microplastics directly into the nearby soil and river due to the lack of proper liner installation [15]. The uncontrolled microplastics ultimately can be reached plants, animals, and humans through the food chain [16-19]. Incineration allows the rapid volume reduction of solid waste through burning

<sup>†</sup>To whom correspondence should be addressed.

E-mail: jechanlee@skku.edu

<sup>‡</sup>These authors are co-first authors because they contributed equally to this work.

Copyright by The Korean Institute of Chemical Engineers.

the waste at high temperatures [20]. However, the emission of greenhouse gases (i.e., CO<sub>2</sub>) and toxic chemicals (unburned hydrocarbons, dioxin, etc.) becomes problematic environmentally [21]. To avoid the environmental issue, air pollution control systems are required [22]. Incineration also can produce heat energy through the oxidation of carbon and hydrogen rich organic waste materials [23]. When the incinerator is connected to power plants and electrical grids, the heat energy can be used as electrical energy [24]. However, residents strongly oppose the construction of incinerators, thereby increasing the transportation fee of waste and construction fee of incinerators and electricity grid, not allowing the incinerator energy and cost-efficient facility [25]. As such, it is crucial to investigate environmentally sound methods for disposal of heterogeneous plastic waste to achieve several goals: (1) prevention of microplastic generation, (2) decreasing potential health risk, (3) rapid volume reduction of solid waste, and (4) production of value-added products through the same process. Such technical platforms can help to minimize the waste generation and provide economic feasibility to the society [26].

In these rationales, thermocatalytic upgrading of disposal wipes is suggested in this study. The thermocatalytic process can convert biomass and plastic waste into value-added (oxygenated) hydrocarbons (HCs) and syngas with rapid conversion of solid plastic mixture [27-33]. A majority of previous research on plastic pyrolysis has focused on upcycling of a single plastic component such as polyethylene and polypropylene rather than practical plastic waste [34-39]. However, thermocatalytic upgrading of disposable wet wipes was rarely investigated though their large production and environmental problems as mentioned above. Pyrolysis of disposable wipes was performed with supported Ni catalyst (Ni/Al<sub>2</sub>O<sub>3</sub>) and non-catalytic pyrolysis was performed as a reference to understand resulting products from thermal degradation of disposable wet wipes. Supported Ni catalyst was employed as a catalyst due to its affordability, accessibility, and uniform dispersion of nano-sized Ni metal on the porous support. Three phase products were analyzed quantitatively. Prior to pyrolysis experiments, chemical composition of disposable wipes was identified through multiple analytical tools. Lastly, the reusability of catalyst was tested.

## EXPERIMENTAL

### 1. Waste Sampling and Characterization

Disposable wipes were bought from a convenience store near Sungkyunkwan University campus (Suwon, Korea) and used to clean different material surfaces such as tables, hands, electronic equipment, etc. The spent disposable wipes were washed with deionized water and then dried in a drying oven at 60 °C for 24 h. The spent wipes were cut and shredded to make small sized samples (<10 mm<sup>2</sup>) for characterization. Proximate analysis of the spent disposable wipes employed three different temperature programs in a muffle furnace: (1) drying at 105 °C for 24 h to measure the moisture content, (2) heating the sample up to 450 °C and the remaining for 1 h at 450 °C to measure volatile matter content, and (3) heating the sample to 750 °C for 1 h to measure the ash and fixed matter. Moisture, volatile matter, fixed matter, and ash contents were calculated gravimetrically. Ultimate analysis was performed to quan-

tify the C, H, N, and S contents in the spent disposal wipes using the elemental analyzer (TRSMCHNSC - 6280TRSM, LECO, USA). Oxygen (O) content was estimated by subtracting other elements and ash contents measured. Thermal degradation characteristics of the spent disposal wipes were monitored using thermogravimetric analysis (TGA). The instrument used was a thermal analyzer-mass spectrometer coupling (STA 409 PC+QMS 403 C, NETZSCH, Germany). Temperature program started from room temperature and ended at 900 °C with a heating rate of 10 °C min<sup>-1</sup>. Fourier-transform infrared spectroscopy (Nicolet iS50, Thermo Fisher Scientific, USA) was performed to determine the chemical composition of the spent disposable wipes.

### 2. Catalyst Synthesis

Incipient wetness impregnation was employed to disperse Ni catalyst on alumina support (10 wt% Ni supported on alumina: Ni/Al<sub>2</sub>O<sub>3</sub>). Powdered nickel nitrate hexahydrate (Ni(NO<sub>3</sub>)<sub>2</sub>·6H<sub>2</sub>O) and aluminum oxide (Al<sub>2</sub>O<sub>3</sub>; product no. 199443) were purchased from Sigma-Aldrich (USA). Both Ni precursor and alumina (5 to 9 ratio by mass) were mixed with deionized water, and the mixture was stirred for 6 h. Then the sample was dried at 105 °C in the muffle furnace overnight. The resultant was calcined at 500 °C for 4 h, and the heating rate from temperature was 10 °C min<sup>-1</sup>. The calcined one was then reduced at 700 °C for 2 h under different flow gases: (1) 10 vol% H<sub>2</sub> (N<sub>2</sub> balanced) or (2) 10 vol% H<sub>2</sub> (CO<sub>2</sub> balanced). The Ni catalyst reduced under N<sub>2</sub> balanced H<sub>2</sub> gas was denoted as Ni/Al<sub>2</sub>O<sub>3</sub>-N<sub>2</sub>, while the catalyst reduced under CO<sub>2</sub> balanced gas was denoted as Ni/Al<sub>2</sub>O<sub>3</sub>-CO<sub>2</sub>. After the reduction, each catalyst was cooled to room temperature in high purity N<sub>2</sub> purging gas, and then the catalyst passivation was followed for 6 h under 2 vol% O<sub>2</sub> gas (N<sub>2</sub> balanced). The passivated catalysts were used for pyrolysis of spent disposable wipes after characterizations.

### 3. Catalyst Characterization

The two Ni/Al<sub>2</sub>O<sub>3</sub> catalysts were characterized by N<sub>2</sub> physisorption to determine surface area, pore volume, and average pore diameter. The number of surface metallic Ni sites (in terms of H<sub>2</sub> uptake) was determined by H<sub>2</sub> chemisorption. An adsorption analyzer (ASAP 2020 Plus, Micromeritics, USA) was used for conducting N<sub>2</sub> physisorption and H<sub>2</sub> chemisorption. X-ray diffraction (XRD) analysis of the two catalysts was carried out using an X-ray diffractometer (D8 Discover, Bruker, USA). The TGA of reused catalyst samples was performed using the same instrument that characterize the feedstock sample (Section 2.1).

### 4. Reactor Setup

Fixed bed reactors were constructed for pyrolysis of spent disposable wipes, and a heating furnace covered the outer surface of reactor to supply heat energy for pyrolysis experiments. 800 mm long quartz cylinder was used as a reactor body to place disposable wipe on its center. One layer of the spent wipe was used as a feedstock for pyrolysis experiments. In catalytic pyrolysis, Ni/Al<sub>2</sub>O<sub>3</sub>-N<sub>2</sub> or Ni/Al<sub>2</sub>O<sub>3</sub>-CO<sub>2</sub> was used as a catalyst, and the mass ratio of feedstock to catalyst was 1 to 1. The catalyst bed was located next to the feedstock bed in the tubular reactor to make ex situ pyrolysis setup. Before pyrolysis tests, N<sub>2</sub> gas (100 mL min<sup>-1</sup>) flowed into the reactor for 20 min to remove air and moisture. Then, the temperature program started from room temperature to 800 °C for pyrolysis of spent wipes. After pyrolysis temperature was reached,

pyrolysis was performed at the final temperature for 1 min and then heating furnace was turned off. For the evaluation of catalyst stability, Ni/Al<sub>2</sub>O<sub>3</sub>-N<sub>2</sub> was used as a catalyst after regeneration (three times). Used Ni/Al<sub>2</sub>O<sub>3</sub>-N<sub>2</sub> catalyst was heated to 650 °C (heating rate: 10 °C min<sup>-1</sup>) and held for 1 h under the low concentration of O<sub>2</sub> stream (N<sub>2</sub>:air=9:1 by mass) for regeneration. After that, the used Ni/Al<sub>2</sub>O<sub>3</sub>-N<sub>2</sub> catalyst was reduced under 10 vol% H<sub>2</sub> gas (N<sub>2</sub> condition) as described in Section 2.2. to be used as regenerated Ni catalyst for catalytic pyrolysis. All the pyrolysis experiments were performed at least three times, and the error bar was less than 2%.

### 5. Product Analysis

Different products (char, wax, liquid, and gaseous pyrolysates) were analyzed using multiple chromatography instruments and elemental analyzer. Volatile matters generated from the pyrolysis reactor were captured through consecutive cooling traps connected to the pyrolysis reactor. The first cooling stage was made of ice bath connected with a circulating chiller working at -1 °C, and the following cooling stage was dry ice and acetone bath, whose temperature was -50 °C. This setup was aimed to capture condensable volatile matter, namely pyrolysis oil. To analyze the chemical composition of the pyrolysis oil, the condensable sample was injected into a gas chromatograph-mass spectrometer (Agilent 8890 MS 5977B, USA). Detailed instrument program is described in Supporting Information (Table S1). The concentration of each chemical species was calculated by applying the internal standard method using 5-methylfurfural (10 ng mL<sup>-1</sup>). Non-condensable volatile mat-

ter directly flowed into an online micro-GC (INFICON Fusion, Switzerland). Detailed measurement condition of micro-GC is shown in Table S2. Solid product (plastic char), solid residue remained after pyrolysis, was gravimetrically measured. Wax-like compound was calculated by subtracting the mass of liquid, gas, and solid from the original mass of feedstock.

## RESULTS AND DISCUSSION

### 1. Characterization of Spent Disposable Wipe Feedstock

The proximate analysis of the spent disposable wipe sample confirmed that it was composed mainly of volatile matter (81.18 wt%) followed by ash (16.12 wt%), moisture (1.95 wt%), and fixed carbon (0.75 wt%). According to the ultimate analysis of the spent wipe sample, the contents of carbon, oxygen, hydrogen, and sulfur of the spent wipe feedstock were 50.3, 27.29, 5.07, and 1.2 wt% (balance ash), respectively. Nevertheless, the content of nitrogen was negligible (much less than 1 wt%). The compositions of the spent wipe sample are summarized in Table 1.

The FTIR absorption spectrum of the spent disposable wipe sample is shown in Fig. 1(a), which confirmed that the disposable wipe is made of polyester elastomer (Fig. S1). The absorption band associated with the stretching vibration of C-O bond in aliphatic esters (e.g., fatty acid esters) was found at near 1,175 cm<sup>-1</sup> [40]. The adsorption peak at near 1,500 cm<sup>-1</sup> and 1,720 cm<sup>-1</sup> were assigned to in-plane skeletal vibration of benzene ring and carbonyl func-

Table 1. Composition of the spent disposable wipe feedstock obtained by proximate and ultimate analyses

Thermochemical composition (wt%)							
Moisture	Volatile matter			Fixed carbon	Ash	Total	
1.95	81.18			0.75	16.12	100	
Elemental composition (wt%)							
C	H	O	N	S	Ash	Total	
50.3	5.07	27.29	0.02	1.2	16.12	100	

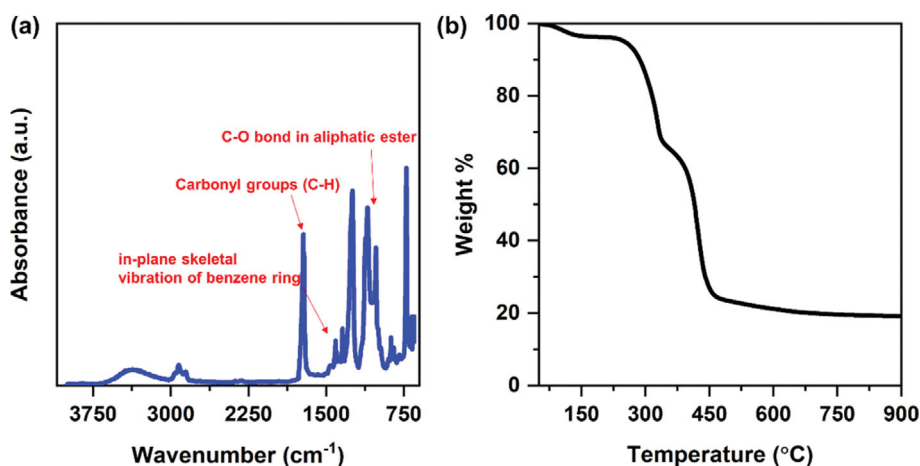


Fig. 1. (a) Infrared absorption spectrum of the spent disposable wipe feedstock obtained by Fourier transform infrared spectroscopy analysis and (b) residual mass change profile of the spent disposable wipe feedstock obtained by thermogravimetric analysis under an N<sub>2</sub> environment.

**Table 2. Physicochemical properties of the fresh and reused Ni/Al<sub>2</sub>O<sub>3</sub>-N<sub>2</sub> and Ni/Al<sub>2</sub>O<sub>3</sub>-CO<sub>2</sub> catalysts**

No.	Catalyst	Surface area (m <sup>2</sup> g <sup>-1</sup> )		Pore volume (cm <sup>3</sup> g <sup>-1</sup> )			Average pore diameter <sup>c</sup> (nm)	H <sub>2</sub> uptake <sup>d</sup> (μmol g <sup>-1</sup> )
		BET	External <sup>a</sup>	Micro <sup>a</sup>	Meso <sup>b</sup>	Total <sup>c</sup>		
1	Ni/Al <sub>2</sub> O <sub>3</sub> -N <sub>2</sub>	112.68	112.48	0.217	0.004	0.221	5.55	2.61
2	Ni/Al <sub>2</sub> O <sub>3</sub> -CO <sub>2</sub>	105.65	104.73	0.216	0.003	0.219	5.69	0.03
3	Ni/Al <sub>2</sub> O <sub>3</sub> -N <sub>2</sub> (1 <sup>st</sup> reuse)	104.79	89.38	0.189	0.003	0.192	6.34	4.39
4	Ni/Al <sub>2</sub> O <sub>3</sub> -N <sub>2</sub> (2 <sup>nd</sup> reuse)	99.69	87.71	0.189	0.003	0.192	6.30	4.55

<sup>a</sup>Determined by the t-plot method.

<sup>b</sup>Calculated by subtracting micropore volume from total pore volume.

<sup>c</sup>Determined by the Barrett-Joyner-Halenda (BJH) desorption method at a relative pressure (P/P<sub>0</sub>) of 0.99.

<sup>d</sup>Measured using the H<sub>2</sub> chemisorption method under a static condition at 35 °C.

tionalities (C-H), respectively [40]. Fig. 1(b) presents thermal degradation trend of the spent disposable wipe sample. Until 110 °C, ~2 wt% of the spent disposable wipe sample was degraded due to the evaporation of moisture (Table 1). Approximately 80 wt% of the sample was further decomposed until ~500 °C, consistent with the content of volatile matter (Table 1). Residual weight percent was ~18 wt%, which could be composed of fixed carbon and ash.

## 2. Characterization of Ni/Al<sub>2</sub>O<sub>3</sub> Catalysts

Table 2 lists the physicochemical properties of the two Ni catalysts made under two different atmospheres (N<sub>2</sub> and CO<sub>2</sub>) before and after use. The Ni/Al<sub>2</sub>O<sub>3</sub>-N<sub>2</sub> had a Brunauer-Emmett-Teller (BET) specific surface area of 112.68 m<sup>2</sup> g<sup>-1</sup> that was about 7% higher than that of the Ni/Al<sub>2</sub>O<sub>3</sub>-CO<sub>2</sub>. The atmosphere in which the catalyst was treated during its preparation did not have a significant effect on the pore volume and average pore size. However, the Ni catalyst treated in N<sub>2</sub> environment exhibited an 86-fold higher H<sub>2</sub> uptake than the Ni catalyst treated in CO<sub>2</sub> environment, indicating that the treatment of Ni/Al<sub>2</sub>O<sub>3</sub> under N<sub>2</sub> resulted in a higher number of surface metallic Ni sites than the treatment under CO<sub>2</sub>. This is probably because the reverse water gas shift (RWGS) reaction, which theoretically converts 85.8% H<sub>2</sub> and 9.5% CO<sub>2</sub> to H<sub>2</sub>O and CO at 700 °C, is accompanied by H<sub>2</sub> reduction under 10% H<sub>2</sub> and 90%

CO<sub>2</sub>, based on the equilibrium composition calculations of HSC Chemistry 9 (Qutotec). Coke formation is not possible under these treatment conditions. The presence of 90% CO<sub>2</sub> in the treatment gas at 700 °C allows metallic Ni to theoretically balance 3.1% NiO and 0.2% NiAl<sub>2</sub>O<sub>4</sub>, but their presence is negligible in the presence of 90% N<sub>2</sub>. Note that the NiAl<sub>2</sub>O<sub>4</sub> formation is possible during the calcination of the Ni/Al<sub>2</sub>O<sub>3</sub> catalyst, but this possibility was not considered in our estimation. The characterization results indicate that the variation in atmosphere where the Ni/Al<sub>2</sub>O<sub>3</sub> catalyst treatment took place (e.g., N<sub>2</sub> or CO<sub>2</sub>) may alter its physicochemical properties, particularly affecting its H<sub>2</sub> uptake.

The XRD patterns of the Ni/Al<sub>2</sub>O<sub>3</sub>-N<sub>2</sub> and Ni/Al<sub>2</sub>O<sub>3</sub>-CO<sub>2</sub> catalysts are shown in Fig. 2. The diffraction peaks of the two catalysts are almost identical and represent clear peaks of metallic Ni and Al<sub>2</sub>O<sub>3</sub>, which were identified according to the International Centre for Diffraction Data database. In addition, the Ni/Al<sub>2</sub>O<sub>3</sub>-N<sub>2</sub> and Ni/Al<sub>2</sub>O<sub>3</sub>-CO<sub>2</sub> catalysts exhibits a similar XRD intensity, which means that both catalysts have a similar degree of crystallinity.

## 3. Thermocatalytic Conversion of Spent Disposable Wipes over Ni/Al<sub>2</sub>O<sub>3</sub> Catalysts

Fig. 3 shows the yields for gas and liquid pyrolysates and other byproducts (e.g., wax char) obtained through the thermocatalytic conversion of the spent disposable wipe feedstock with and without the Ni/Al<sub>2</sub>O<sub>3</sub>-N<sub>2</sub> and Ni/Al<sub>2</sub>O<sub>3</sub>-CO<sub>2</sub> catalysts. The use of the Ni catalysts markedly influenced the yields of gas pyrolysate and wax.

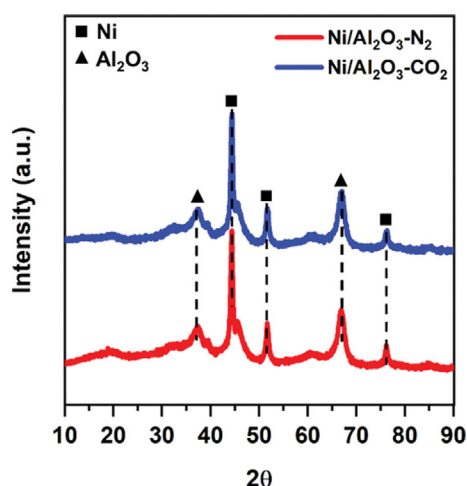


Fig. 2. X-ray diffraction patterns of the Ni/Al<sub>2</sub>O<sub>3</sub>-N<sub>2</sub> and Ni/Al<sub>2</sub>O<sub>3</sub>-CO<sub>2</sub> catalysts.

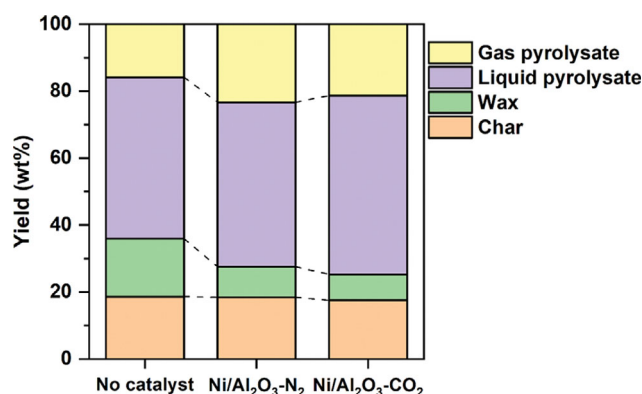


Fig. 3. Mass balance of the pyrolysates of the spent disposable wipe feedstock obtained with and without the Ni/Al<sub>2</sub>O<sub>3</sub> catalysts.

Note that the wax is a mixture of long-chain aliphatic HCs that exist as sticky form between liquid and solid phase product. It included  $\geq C_{20}$  HCs, but unable to fully identify its composition because GC does not allow the analysis of high molecular weight compounds. The two catalysts increased the yield of gas pyrolysate while they decreased the yield of wax. Gas pyrolysate is typically a mixture of non-condensable gases (i.e.,  $H_2$ , CO,  $CO_2$ ,  $C_1$ - $C_4$  hydrocarbons) and wax is generally composed of heavy molecules of  $C_{>20}$  [41]. This clearly means that the two  $Ni/Al_2O_3$  catalysts enhanced thermal cracking of high-molecular-weight compounds into low-molecular-weight compounds (e.g., non-condensable gases). Nevertheless, the use of the Ni catalysts had no significant impact on the yields of liquid pyrolysate and char, compared to the non-catalytic thermal conversion of the spent disposable wipe feedstock. The  $Ni/Al_2O_3-N_2$  catalyst led to a higher yield of gas pyrolysate and a less yield of wax than the  $Ni/Al_2O_3-CO_2$  catalyst, indicating that the  $Ni/Al_2O_3-N_2$  catalyst was more effective at thermal cracking of heavy compounds during the thermal conversion of the spent disposable wipe feedstock. This could be ascribed to more surface Ni sites available on the  $Ni/Al_2O_3-N_2$  catalyst because Ni is effective at promoting C-C bond scission [42].

In Fig. 4(a), the distributions of chemical compounds identified in the liquid pyrolysate of the spent disposable wipe feedstock obtained with and without the two different Ni catalysts are compared. Benzoic acid and its derivatives (e.g., acetyl benzoic acid, methylbenzoic acid, ethylbenzoic acid, and formylbenzoic acid) accounted for >80% of the liquid pyrolysate for all cases. This was most likely due to the benzene ring existing in the polyester structure of the disposable wipe sample (Fig. 1(a)). Other than them, terephthalic acid, biphenyls, and 9H-fluorenes were identified as constituents

of the liquid pyrolysate. The atmosphere in which a  $Ni/Al_2O_3$  catalyst was treated did not considerably affected the product distribution of the liquid pyrolysate.

Fig. 4(b) compares the product distribution of the gas pyrolysate produced from the spent disposable wipe feedstock with and without the  $Ni/Al_2O_3$  catalysts. As mentioned, the gas pyrolysate consisted of different permanent gases including  $H_2$ , CO,  $CO_2$ ,  $CH_4$ , and  $C_2$ - $C_4$  hydrocarbons. A clear pattern was observed: the  $Ni/Al_2O_3-N_2$  catalyst led to the production of more  $H_2$  and less  $CO_2$  than no catalyst and the  $Ni/Al_2O_3-CO_2$  catalyst. For example, the thermocatalytic conversion of the spent disposable wipe feedstock over the  $Ni/Al_2O_3-N_2$  catalyst produced 102% higher  $H_2$  than the non-catalytic thermal conversion of the spent disposable wipe feedstock. A 36.9% more  $H_2$  was produced with the  $Ni/Al_2O_3-N_2$  catalyst in comparison with the  $Ni/Al_2O_3-CO_2$  catalyst. It has been known that Ni serves as an active catalytic site for cleavage of O-H, C-C, and C-H bonds and water-gas shift reaction, thereby promoting  $H_2$  production from organic compounds [43-49]. As seen in Table 1, the  $Ni/Al_2O_3-N_2$  catalyst had more surface Ni sites than the  $Ni/Al_2O_3-CO_2$  catalyst. The higher number of surface Ni sites on the  $Ni/Al_2O_3-N_2$  catalyst should contribute to yielding more  $H_2$  from the spent disposable wipe feedstock. Nonetheless, the gas pyrolysate produced in the presence of the  $Ni/Al_2O_3-N_2$  catalyst contained 23.8 mol%  $CO_2$ , while that produced in the presence of the  $Ni/Al_2O_3-CO_2$  catalyst contained 27.9 mol%  $CO_2$ .

Elemental composition of the char retained after the thermocatalytic conversion of the spent disposable wipe feedstock was determined in order to estimate energy content of the char, as summarized in Table 3. The char obtained in the presence of the  $Ni/Al_2O_3-N_2$  catalyst contained less carbon than others. This is most

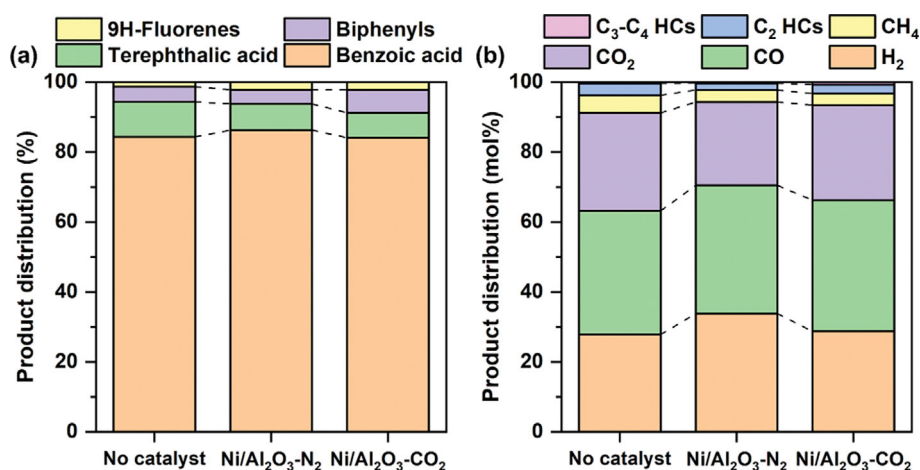


Fig. 4. Product distribution identified in (a) liquid pyrolysate and (b) gas pyrolysate of the spent disposable wipe feedstock obtained with and without the  $Ni/Al_2O_3$  catalysts.

Table 3. Elemental composition (wt%) of the chars made with and without the  $Ni/Al_2O_3-N_2$  and  $Ni/Al_2O_3-CO_2$  catalysts

Catalyst	C	H	O	N	S	Ash	Total
No catalyst	80.68	0.91	6.43	0.40	0.34	11.24	100
$Ni/Al_2O_3-N_2$	77.87	0.74	6.37	0.49	0.28	14.25	100
$Ni/Al_2O_3-CO_2$	85.52	0.69	5.99	0.40	0.29	7.11	100

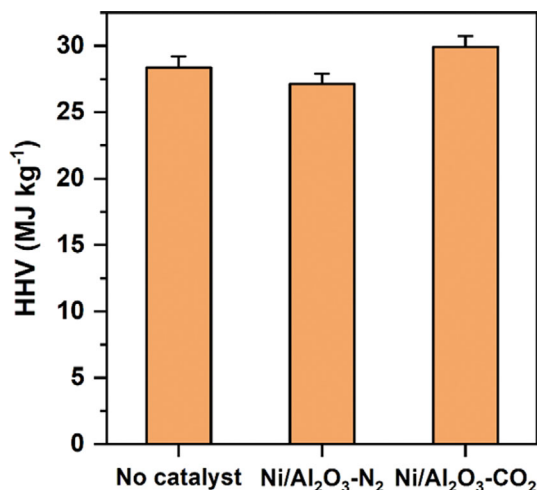


Fig. 5. Higher heating value (HHV) of the chars made with and without the Ni/Al<sub>2</sub>O<sub>3</sub>-N<sub>2</sub> and Ni/Al<sub>2</sub>O<sub>3</sub>-CO<sub>2</sub> catalysts.

likely because the Ni/Al<sub>2</sub>O<sub>3</sub>-N<sub>2</sub> catalyst led to releasing more gaseous products from the spent disposable wipe feedstock (Fig. 3). Higher heating values (HHVs) of three different chars are compared in Fig. 5, estimated based on their elemental compositions (Table 3) using an empirical equation [50]. The char made with the Ni/Al<sub>2</sub>O<sub>3</sub>-N<sub>2</sub> catalyst exhibited the lowest HHV, likely attributed to the lowest carbon content among the three.

As discussed above, the use of the Ni/Al<sub>2</sub>O<sub>3</sub>-N<sub>2</sub> catalyst resulted in the highest H<sub>2</sub> yield among three cases (Figs. 3 and 4). Thus, to evaluate reusability of the Ni/Al<sub>2</sub>O<sub>3</sub>-N<sub>2</sub> catalyst in terms of H<sub>2</sub> production from the spent wipes, the Ni/Al<sub>2</sub>O<sub>3</sub>-N<sub>2</sub> catalyst was used for three cycles (Fig. 6(a)). Fig. 6(a) presents a slight loss in the H<sub>2</sub> yield after each use of the catalyst. As seen in Table 2 (Nos. 1, 3, and 4), the reuse of the catalyst decreased its surface area and total pore volume. The decrease in surface area and pore volume can be attributed to the deposition of carbon onto the catalyst surface,

as observed in the TGA analysis result of the reused catalysts (Fig. 6(b)). The decrease in the sample mass found between 400 and 800 °C was ascribed to the oxidation of the deposited carbon [51]. Fig. 6(b) also shows that more carbon was deposited onto the catalyst surface as the number of reuse cycle was increased. Unlike surface area and pore volume, H<sub>2</sub> uptake was increased after the use of the Ni/Al<sub>2</sub>O<sub>3</sub>-N<sub>2</sub> catalyst (No. 1, 3, and 4 in Table 2). The increase in the H<sub>2</sub> uptake was most likely due to the redispersion of Ni species that interact less with the surface alumina upon reduction by hydrocarbons in the disposable wipe feedstock under the reaction conditions (refer Section 2.4). This trend can occur when the nickel species in alumina are covered or submerged by NiAl<sub>2</sub>O<sub>4</sub> [52]. Thus, the loss in the H<sub>2</sub> yield was ascribed to the carbon deposition. In spite of the loss in the H<sub>2</sub> yield, no significant decrease in the H<sub>2</sub> yield was exhibited based on the Student's t-test (confidence limit: 95%).

Transition metal catalysts have a high probability of producing H<sub>2</sub> from plastic pyrolysis due to their capability for C-C and C-H bond scissions, but Ni catalyst was only tested in this study. Therefore, it will be important for future studies to develop highly efficient transition metal catalysts that can enhance H<sub>2</sub> yield and production rate at lower pyrolysis temperature.

## CONCLUSIONS

The present study was aimed specifically at upcycling of the world-most generated MSW, spent disposable wipes, through thermocatalytic conversion process over Ni/Al<sub>2</sub>O<sub>3</sub> catalysts prepared under different atmospheres such as N<sub>2</sub> and CO<sub>2</sub>. The two catalysts exhibited different physicochemical properties, in particular the number of surface Ni sites: the Ni/Al<sub>2</sub>O<sub>3</sub>-N<sub>2</sub> catalyst had 86 times higher H<sub>2</sub> uptake than the Ni/Al<sub>2</sub>O<sub>3</sub>-CO<sub>2</sub> catalyst. The higher number of Ni sites that can be involved in the reaction led to a higher yield of gaseous H<sub>2</sub> from the spent disposable wipe feedstock along with suppressing the formation of byproduct such as wax. However, the

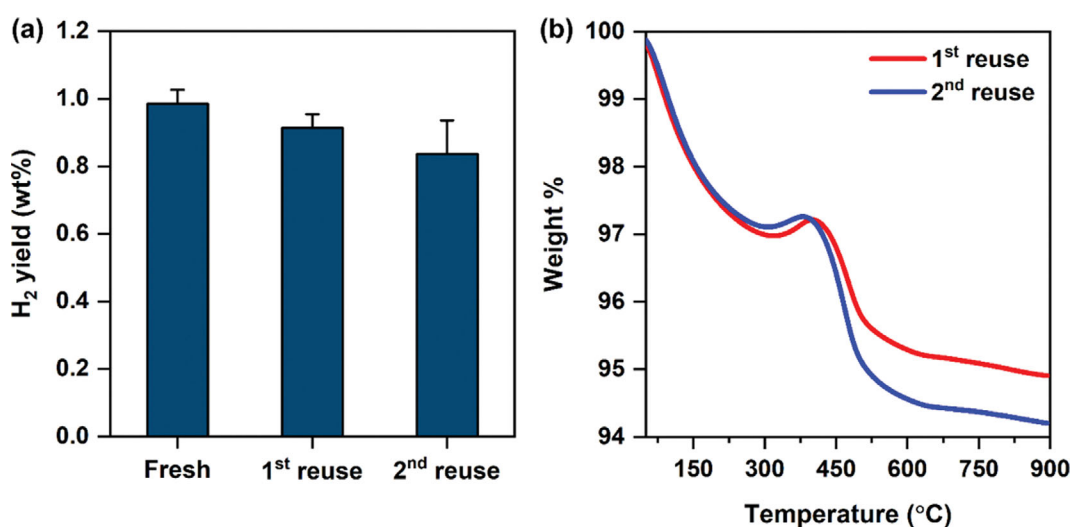


Fig. 6. (a) H<sub>2</sub> yield resulting from the thermocatalytic conversion of the spent disposable wipe feedstock with the Ni/Al<sub>2</sub>O<sub>3</sub>-N<sub>2</sub> catalyst for three cycles and (b) residual mass change profile of the reused Ni/Al<sub>2</sub>O<sub>3</sub>-N<sub>2</sub> catalyst obtained by thermogravimetric analysis under an air environment.

use of the Ni/Al<sub>2</sub>O<sub>3</sub>-N<sub>2</sub> catalyst resulted in the char having the lower HHV than the char made without any catalyst or with the Ni/Al<sub>2</sub>O<sub>3</sub>-CO<sub>2</sub> catalyst, due to its lower carbon content. In sum, this study revealed that the catalyst preparation condition can influence the yield of pyrolysates and the product distribution and energy content of the pyrolysates produced through thermocatalytic conversion of MSW such as spent disposable wipes.

### ACKNOWLEDGEMENTS

This work was supported by the National Research Foundation of Korea (NRF) grant funded by the Korea government (Ministry of Science and ICT; MSIT) (No. 2021R1A4A1031357). This research was also supported by the C1 Gas Refinery Program through the NRF funded by the Korea government (MSIT) (No. 2017M3D3A1A01037001).

### SUPPORTING INFORMATION

Additional information as noted in the text. This information is available via the Internet at <http://www.springer.com/chemistry/journal/11814>.

### REFERENCES

1. Y. Zhang, Z. Wen, Y. Hu and T. Zhang, *J. Clean. Prod.*, **364**, 132684 (2022).
2. T. Hu, M. Shen and W. Tang, *Environ. Sci. Pollut. Res.*, **29**, 284 (2022).
3. Y. Zhang, Z. Wen, W. Lin, Y. Hu, V. Kosajan and T. Zhang, *Resour. Conserv. Recycl.*, **174**, 105803 (2021).
4. H. Xing, A. R. Krogmann, C. Vaught and E. Chambers, *Cosmetics*, **6**, 44 (2019).
5. Grand View Research, Wet wipes market size, <https://www.grandviewresearch.com/industry-analysis/wet-wipes-market-report> (accessed 21 February, 2023).
6. J. N. Hahladakis and E. Iacovidou, *Sci. Total Environ.*, **630**, 1394 (2018).
7. J. Lee, S. Jeong and K.-J. Chae, *Sci. Total Environ.*, **784**, 147144 (2021).
8. M. I. Romero-Gómez, M. A. Pedreño-Rojas, F. Pérez-Gálvez and P. Rubio-de-Hita, *J. Build. Eng.*, **34**, 101874 (2021).
9. R.-L. Mitchell, M. Gunkel, J. Waschnewski and P.U. Thamsen, "Nonwoven wet wipes can be hazardous substances in wastewater systems—evidences from a field measurement campaign in Berlin, Germany", *Frontiers in Water-Energy-Nexus—Nature-Based Solutions, Advanced Technologies and Best Practices for Environmental Sustainability*, Springer International Publishing, Cham, pp. 313-316 (2020).
10. V. C. Shruti, F. Pérez-Guevara and G. Kuttralam-Muniasamy, *Environ. Challeng.*, **5**, 100267 (2021).
11. A. L. P. Silva, J. C. Prata, A. C. Duarte, A. M. V. M. Soares, D. Barceló and T. Rocha-Santos, *Case Stud. Chem. Environ. Eng.*, **3**, 100072 (2021).
12. N. P. Ivleva, A. C. Wiesheu and R. Niessner, *Angew. Chem. Int. Ed.*, **56**, 1720 (2017).
13. O. Ó. Briain, A. R. Marques Mendes, S. McCarron, M. G. Healy and L. Morrison, *Water Res.*, **182**, 116021 (2020).
14. A. Allen, *Eng. Geol.*, **60**, 3 (2001).
15. V. Ishchenko, *Int. J. Environ. Waste Manag.*, **20**, 66 (2017).
16. P. K. Rai, J. Lee, R. J. C. Brown and K.-H. Kim, *J. Clean. Prod.*, **291**, 125240 (2021).
17. T. S. M. Amelia, W. M. A. W. M. Khalik, M. C. Ong, Y. T. Shao, H.-J. Pan and K. Bhubalan, *Prog. Earth Planet. Sci.*, **8**, 12 (2021).
18. K. Duraisamy, R. Ismailgani, S. A. Paramasivam, G. Kaliyaperumal and D. Dillikannan, *Energy Environ.*, **32**, 481 (2021).
19. P. K. Rai, J. Lee, R. J. C. Brown and K.-H. Kim, *J. Hazard. Mater.*, **403**, 123910 (2021).
20. R. V. Moharir, P. Gautam and S. Kumar, "Waste treatment processes/technologies for energy recovery", *Current developments in biotechnology and bioengineering*, Kumar, S., Kumar, R. and Pandey, A., eds., Elsevier, pp. 53-77 (2019).
21. Y. Lee, S. Kim, E. E. Kwon and J. Lee, *J. CO<sub>2</sub> Util.*, **36**, 76 (2020).
22. J. Vehlow, *Waste Manage.*, **37**, 58 (2015).
23. L. Makarichi, W. Jutidamrongphan and K.-a. Techato, *Renew. Sust. Energ. Rev.*, **91**, 812 (2018).
24. R. R. Schmidt, O. Pol, D. Basciotti and J. Page, *EPJ Web of Conferences*, **33**, 04002 (2012).
25. A. A. Patil, A. A. Kulkarni and B. B. Patil, *J. Comput. Technol.*, **3**, 12 (2014).
26. S. Huysman, J. De Schaepe meester, K. Ragaert, J. Dewulf and S. De Meester, *Resour. Conserv. Recycl.*, **120**, 46 (2017).
27. J.-Y. Kim, H. W. Lee, S. M. Lee, J. Jae and Y.-K. Park, *Bioresour. Technol.*, **279**, 373 (2019).
28. H. W. Ryu, D. H. Kim, J. Jae, S. S. Lam, E. D. Park and Y.-K. Park, *Bioresour. Technol.*, **310**, 123473 (2020).
29. S. Pyo, Y.-M. Kim, Y. Park, S. B. Lee, K.-S. Yoo, M. A. Khan, B.-H. Jeon, Y. J. Choi, G. H. Rhee and Y.-K. Park, *J. Ind. Eng. Chem.*, **103**, 136 (2021).
30. M. W. Seo, S. H. Lee, H. Nam, D. Lee, D. Tokmurzin, S. Wang and Y.-K. Park, *Bioresour. Technol.*, **343**, 126109 (2022).
31. D. Lee, H. Nam, M. W. Seo, S. H. Lee, D. Tokmurzin, S. Wang and Y.-K. Park, *Chem. Eng. J.*, **447**, 137501 (2022).
32. S. Valizadeh, H. Hakimian, A. Farooq, B.-H. Jeon, W.-H. Chen, S. H. Lee, S.-C. Jung, M. W. Seo and Y.-K. Park, *Bioresour. Technol.*, **365**, 128143 (2022).
33. O. A. Qamar, F. Jamil, M. Hussain, A. a. H. Al-Muhtaseb, A. Inayat, A. Waris, P. Akhter and Y.-K. Park, *Chem. Eng. J.*, **454**, 140240 (2023).
34. S. M. Al-Salem, A. Antelava, A. Constantinou, G. Manos and A. Dutta, *J. Environ. Manage.*, **197**, 177 (2017).
35. J. Lee, E. E. Kwon, S. S. Lam, W.-H. Chen, J. Rinklebe and Y.-K. Park, *J. Clean. Prod.*, **321**, 128989 (2021).
36. C. Park, N. Lee, I. S. Cho, B. Ahn, H. K. Yu and J. Lee, *Korean J. Chem. Eng.*, **39**, 3343 (2022).
37. W. Yang, K.-H. Kim and J. Lee, *J. Clean. Prod.*, **376**, 134292 (2022).
38. C. Park, H. Lee, N. Lee, B. Ahn and J. Lee, *J. Hazard. Mater.*, **440**, 129825 (2022).
39. S. Kim, W. Yang, H. S. Lee, Y. F. Tsang and J. Lee, *J. Clean. Prod.*, **372**, 133763 (2022).
40. Y. Nagai, T. Ogawa, L. Yu Zhen, Y. Nishimoto and F. Ohishi, *Polym. Degrad. Stab.*, **56**, 115 (1997).

41. N. Lee, K.-Y. A. Lin and J. Lee, *Environ. Res.*, **213**, 113560 (2022).
42. G. Wu, C. Zhang, S. Li, Z. Han, T. Wang, X. Ma and J. Gong, *ACS Sustain. Chem. Eng.*, **1**, 1052 (2013).
43. R. R. Davda, J. W. Shabaker, G. W. Huber, R. D. Cortright and J. A. Dumesic, *Appl. Catal. B: Environ.*, **56**, 171 (2005).
44. S. Adhikari, S. Fernando and A. Haryanto, *Energy Fuels*, **21**, 2306 (2007).
45. B. Zhang, X. Tang, Y. Li, Y. Xu and W. Shen, *Int. J. Hydrog. Energy*, **32**, 2367 (2007).
46. S. Adhikari, S. Fernando and A. Haryanto, *Catal. Today*, **129**, 355 (2007).
47. Y. Cui, V. Galvita, L. Rihko-Struckmann, H. Lorenz and K. Sundmacher, *Appl. Catal. B: Environ.*, **90**, 29 (2009).
48. E. A. Sánchez, M. A. D'Angelo and R. A. Comelli, *Int. J. Hydrog. Energy*, **35**, 5902 (2010).
49. I. Rossetti, A. Gallo, V. Dal Santo, C. L. Bianchi, V. Nichele, M. Signoretto, E. Finocchio, G. Ramis and A. Di Michele, *Chem-CatChem*, **5**, 294 (2013).
50. S. Kim, J. Byun, H. Park, N. Lee, J. Han and J. Lee, *Energy*, **241**, 122876 (2022).
51. H. Zhang, Y. Wang, S. Shao and R. Xiao, *Sci. Rep.*, **6**, 37513 (2016).
52. J. L. Ewbank, L. Kovarik, F. Z. Diallo and C. Sievers, *Appl. Catal. A: Gen.*, **494**, 57 (2015).